Origin of High-Resolution IETS-STM Images of Organic Molecules with Functionalized Tips

Prokop Hapala,[1,*] Ruslan Temirov,[2,3] F. Stefan Tautz,[2,3] and Pavel Jelínek[1,4,†]
[1]Institute of Physics, Academy of Sciences of the Czech Republic, v.v.i., Cukrovarnická 10, 162 00 Prague, Czech Republic
[2]Peter Grünberg Institut (PGI-3), Forschungszentrum Jülich, 52425 Jülich, Germany
[3]Jülich Aachen Research Alliance (JARA)–Fundamentals of Future Information Technology, 52425 Jülich, Germany
[4]Graduate School of Engineering, Osaka University 2-1, Yamada-Oka, Suita, Osaka 565-0871, Japan
(Received 12 September 2014; revised manuscript received 17 October 2014; published 25 November 2014)

Recently, the family of high-resolution scanning probe imaging techniques using decorated tips has been complemented by a method based on inelastic electron tunneling spectroscopy (IETS). The new technique resolves the inner structure of organic molecules by mapping the vibrational energy of a single carbon monoxide (CO) molecule positioned at the apex of a scanning tunneling microscope (STM) tip. Here, we explain high-resolution IETS imaging by extending a model developed earlier for STM and atomic force microscopy (AFM) imaging with decorated tips. In particular, we show that the tip decorated with CO acts as a nanoscale sensor that changes the energy of its frustrated translation mode in response to changes of the local curvature of the surface potential. In addition, we show that high resolution AFM, STM, and IETS-STM images can deliver information about the charge distribution within molecules deposited on a surface. To demonstrate this, we extend our mechanical model by taking into account electrostatic forces acting on the decorated tip in the surface Hartree potential.

DOI: 10.1103/PhysRevLett.113.226101 PACS numbers: 68.37.Ef, 68.37.Ps, 68.43.Fg

One of the most exciting and significant breakthroughs in the field of scanning probe microscopy in the last years is undoubtedly the achievement of high-resolution STM [1] and AFM [2] images of molecular structures with functionalized tips [3–5]. In general, the high-resolution images, being typically acquired in the regime where the tip-surface interaction becomes repulsive, are characterized by the presence of sharp features in both intra- and intermolecular regions. The sharp ridges observed in the intramolecular region often mimic the internal molecular structure [4,6], with only a few exceptions [7,8]. The capability of AFM/STM to resolve internal atomic and chemical structures in real space opened new horizons for the characterization of molecules and surfaces at the atomic scale [6,9–17].

The origin of the high resolution of molecular structures in AFM and STM images has been attributed to Pauli repulsion [2,4,18] and the bending of the functionalized tip apex [6]. Recently, we introduced a simulation model which provides a unified insight into the detailed mechanism of the high-resolution imaging with decorated tips in both AFM and STM [8]. According to the model, the decorated tip apex acts as a nanoscale force sensor that responds with significant relaxations of the decorating particle (probe particle) towards local minima of the tip-sample interaction potential at close distances. These relaxations cause kinks in both the frequency shift and the tunneling current signals and thus become observable in AFM and STM images as sharp contrast features [8]. Although the model of Ref. [8] was originally used to confirm the decisive role of Pauli repulsion in high-resolution STM and AFM imaging of molecular structures with functionalized tips, it must be noted that imaging of other types of interactions (e.g., electrostatic) should also be possible. Namely, the influence of the intramolecular charge distribution [19] on the molecular contrast has not been analyzed in detail yet.

Inelastic electron tunneling spectroscopy (IETS) [20] is a well-established technique, which has been used to perform, e.g., chemical identification [21] or reaction [22–24] and molecular manipulation [25]. Very recently, Chiang *et al.* [26] introduced a novel approach of high-resolution molecular imaging by means of IETS. They obtained high-resolution images of a cobalt-phthalocyanine (CoPc) molecule deposited on the Ag(110) surface by mapping the IETS feature corresponding to the frustrated translation vibrational mode of a CO molecule attached to the STM tip. The IETS-STM maps of Chiang *et al.* show the sharply resolved structure of the molecular skeleton (i.e., the positions of atoms and bonds), very similar to the high-resolution AFM/STM images with functionalized tips [1,2]. Also the constant-height STM image recorded during IETS mapping (see Fig. S4 in Ref. [26]) shows characteristic sharp contrast features similar to those observed in earlier STM experiments [1,4,27]. Further proliferation of the IETS-STM imaging method, as well as the precise interpretation of the experimental results, strongly depends on a detailed understanding of the imaging mechanism. However, the underlying mechanism of the high-resolution IETS-STM images has not been addressed yet.

In this Letter, we provide an explanation of the origin of the high-resolution IETS-STM images of Ref. [26]. We show how the frequency of the frustrated translation mode of the probe particle terminating the tip is influenced by changes of the surface potential. The IETS-STM imaging can thus be seen as another utilization of the nanoscale sensor functionality of the decorated tip [4], mapping the interactions between the tip and the surface and transducing it—in this case—into the characteristic IETS signal. We also extend our AFM/STM simulation model [8] by including the electrostatic force acting on the functionalized probe in the surface Hartree potential. This allows us to analyze in detail the influence of electrostatic forces on high-resolution images. By applying the extended model to the analysis of the IETS-STM images of CoPc/Ag(110) reported by Chiang *et al.* [26], we demonstrate that the decorated tip is also sensitive to the electrostatic interaction between a charge localized on the tip apex and an electrostatic polarization generated by the inhomogeneous charge distribution inside the CoPc molecule.

We start by briefly summarizing the basic ingredients of our mechanical model; for details, see Ref. [8]. A single atom or a small molecule decorating the apex of a metal tip is modeled by a single point particle interacting via van der Waals attraction and Pauli repulsion with the atoms of the surface and the metallic tip apex atom. These interactions are described by empirical pairwise Lennard-Jones (LJ) potentials. The repulsive branch of the LJ potential describes the Pauli repulsion that plays the key role in the high-resolution imaging. Additionally, in order to simulate the cylindrical confinement potential of the tip, the movement of the probe particle is constrained by a lateral harmonic potential below the metallic tip apex. The harmonic potential determines the lateral "bending" stiffness k of the functionalized tip.

On top of the mechanical model we simulate the STM images by computing the tunneling current through the junction at each lateral position of the tip as a two-step tunneling process between the tip and the probe particle and further between the probe particle and the sample. As it has been shown previously [8], our model reproduces all essential features of experimental high-resolution AFM/STM images very well. More details about the model and its comparison with experimental evidence can be found in Ref. [8].

To address the IETS-STM experiments of Ref. [26], we have extended our model to include a calculation of the vibrational energy levels ϵ of the probe particle. In addition, we have included the previously neglected electrostatic force which stems from the Coulombic interaction between the internal charge distribution on a surface or in a molecule and a charge cloud localized on the probe particle. For the detailed description of the new model see the Supplemental Material [28].

For didactic purposes, we first illustrate on a simplified model how the interaction with a surface atom influences vibration modes of the probe particle. In this model the probe particle can move just in one dimension (x_{PROBE}) while it is fixed at a particular distance (z_{PROBE}) from the single atom on the surface. The overall potential felt by the probe particle is given by two contributions: (i) the harmonic potential, which simulates bending stiffness of the probe particle [see V_{SPRING} in Fig. 1(a)] and (ii) the van der Waals and Pauli potentials acting between the probe particle and the surface atom modeled by the LJ potential

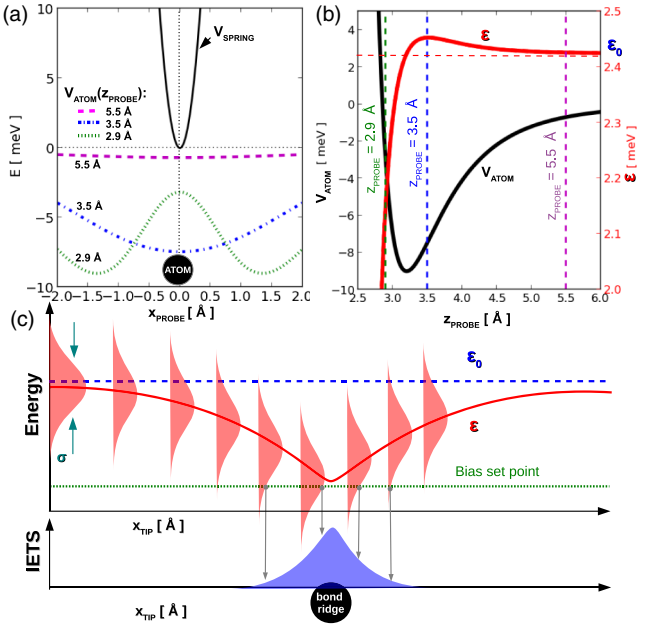

FIG. 1 (color online). 1D IETS-STM model. (a) Individual contributions to the potential energy of the probe particle, plotted as a function of its lateral position x_{PROBE}: The full line shows the harmonic potential of the tip (V_{SPRING}) responsible for the lateral confinement of the probe particle beneath the apex. The dashed lines show the L-J potential of the interaction of the probe particle with the surface atom (V_{ATOM}) or three different distances between probe particle and surface z_{PROBE}= 5.5 Å (pink dashed line), 3.5 Å (blue dash-dot line) and 2.9 Å (green dotted line). (b) Corresponding evolution of the vibration energy eigenvalue ϵ of the probe particle (red line) and probe particle potential energy V_{ATOM} (black line) as a function of z_{PROBE}. Relaxations of the probe particle are not taken into the account in the model. (c) Schematic explanation how the variation of the vibration energy eigenvalue ϵ (red line) affects the intensity of the IETS-STM signal (blue peak) when the tip scans over a surface protrusion (e.g. a bond ridge or an atom). At close tip-surface distances (repulsive regime), the proximity of the surface atom/bond ridge produces a softening of the vibration energy ϵ with respect to the unperturbed vibration energy ϵ_0 (dashed blue line). Thus the characteristic IETS peak [21] (represented by the red gaussian) centered at the vibration energy ϵ crosses the bias set point (green line) at a certain x_{TIP} accordingly changing the IETS-STM signal (blue peak). We used L-J parameters of oxygen atom for both probe particle and surface atom (see [28]) for (a),(b).

[V_{ATOM} in Figs. 1(a) and 1(b)]. For simplicity, the LJ potential between the probe particle and the tip apex atom is neglected in the didactic one-dimensional model; instead, the probe particle is constrained to a fixed z_{PROBE}. Note, however, that in our full 3D simulations this potential is included.

The red line in Fig. 1(b) shows the variation of the vibrational energy ε with the distance z_{PROBE}. In the far distance regime, e.g., at $z_{PROBE} = 5.5$ Å, the interaction with the substrate is negligible. Therefore, the potential affecting the motion of the probe particle is entirely determined by the lateral harmonic potential of the tip. In our simulations we set the stiffness of this potential to $k = 1.44$ N/m. This provides a vibrational energy of the frustrated translation mode of 2.4 meV, which is in good agreement with the experimental observation [26]. The chosen k corresponds well to the upper range predicted for CO-terminated tips (see the supplementary section of Ref. [6]).

At intermediate distances, e.g., $z_{PROBE} = 3.5$ Å, the presence of the attractive surface potential with convex curvature increases slightly the vibration energy ε (by < 0.1 meV). On the other hand, at close distances, e.g., $z_{PROBE} = 2.9$ Å, the surface potential becomes repulsive with a distinct concave curvature near the maximum at the position of the surface atom [see the dashed green line in Fig. 1(a)]. This leads to a considerable softening (by ≈ 0.3 meV) of the vibration energy ε.

If we approach even closer towards the surface atom, the curvature of the total potential would become negative, leading to an unphysical imaginary vibration frequency. At these distances, it is thus necessary to consider the relaxation of the probe particle into a new local minimum to obtain physically meaningful results.

Let us generalize this observation to a 2D situation, where the tip scans in a lateral direction over a molecule at a close distance. In this case, the repulsion and, hence, the concave curvature of the surface potential is highest in areas directly above the molecular skeleton (i.e., local maxima and saddles). Figure 1(c) displays schematically the variation of the frustrated translation vibrational energy ε when the tip moves laterally across a bond or atom of the molecule. We see that ε and, consequently, the position of the IETS peak [29] decrease as the probe particle approaches the bond or atom, with a sharp minimum just above them. Therefore, the lateral mapping of the IETS peak intensity, recorded at a properly selected bias voltage [indicated by the dashed green line in Fig. 1(c)], gives rise to an image contrast that exhibits significant variations over bonds and atoms. This explains why in the experiment bond ridges appear bright in the IETS signal [26]. However, we should stress that in the above analysis we have not yet taken into account the probe particle relaxation. As we will demonstrate later, the probe particle relaxation leads to a considerable sharpening of the IETS-STM contrast, as in the case of high-resolution AFM and STM imaging [6,8] (see also the Supplemental Material [28]).

Now we benchmark our model against experimental results of a CoPc molecule deposited on a Ag(110) surface [26]. First, we carry out total energy DFT calculations with the VASP code in order to obtain an optimized structure of the adsorbed molecule. A detailed description of the DFT calculations can be found in the Supplemental Material [28]. According to the DFT calculations, the molecule is located ≈ 3 Å above the surface and the Co and N atoms bend slightly downward, establishing a chemical bond with Ag atoms underneath. On the other hand, the outer benzene rings move slightly upward so that the molecular buckling is ≈ 0.6 Å.

More importantly, the DFT simulation indicates a substantial charge redistribution within the CoPc molecule. The Hartree potential shown in Fig. 2 reveals a positive potential over the pentagonal pyrrole ring and a negative potential over the imine nitrogens. In order to account for the possible effects caused by the charge redistribution inside CoPc, we extend the original model [8] by including the electrostatic interactions between the probe particle and the surface. The electrostatic force is evaluated from the Hartree surface potential obtained from DFT calculations and a preselected charge density on the probe particle (for details see the Supplemental Material [28]). As will be shown below, the inclusion of electrostatic interactions between the tip and the surface is vital for understanding the experimental IETS-STM contrast.

A detailed analysis of the experimental IETS-STM images of the CoPc molecule reveals an enlargement of the pyrrole rings together with a contraction of the area corresponding to the imine nitrogens in the central part of

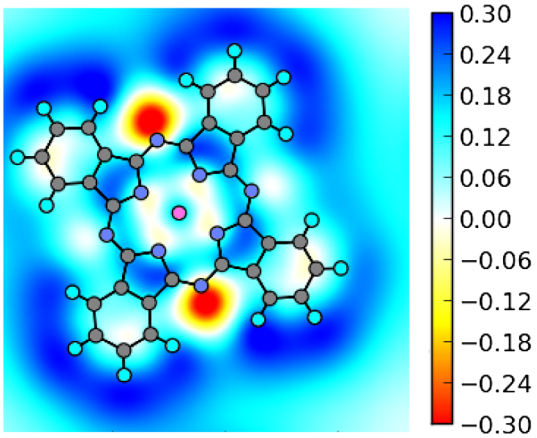

FIG. 2 (color online). Hartree potential of a CoPc molecule adsorbed on Ag(110), obtained from DFT calculations in the xy plane 2.00 Å above the Co atom of the molecule. The Hartree potential reveals substantial partial charging between the pyrrole rings and imine nitrogens. Color scale bar in eV. The following color code for atoms is used: N: blue, C: gray, H: turquoise, Co: pink.

the molecule (see Fig. 3 in Ref. [26]). This is the area where the Hartree potential rapidly changes its sign (see Fig. 2). Figure 3 shows our simulated constant-height IETS-STM images obtained with the extended simulation model, including the electrostatic interactions for different values of charge located on the probe particle. We see that the inclusion of the electrostatic interaction distorts the molecular contrast in the central part of the molecule (the red line in Fig. 3 depicts the molecular skeleton of the relaxed molecule). The calculated IETS-STM image [Fig. 3(a)] obtained with the negatively charged probe particle $Q = -0.4e$ matches very well the experimental evidence (compare to Fig. 3A in Ref. [26]). Alternatively, the presence of the positive charge $Q = +0.4e$ on the probe particle leads to an opposite effect as visible in Fig. 3.

We note that our simulated constant-height IETS-STM images display a more pronounced contrast on the outer benzene rings compared to the experiment [26]. This discrepancy can be explained by the large flexibility of the outer benzene rings. According to our DFT simulations, the benzene rings are only weakly coupled to the silver surface. Thus, when the tip operates in the repulsive regime, one can expect the flexible benzene rings of CoPc to bend down under the force exerted by the tip. We assume this bending to be responsible for the reduced resolution over the benzene rings in the experiment. In the IETS-STM simulation, in contrast, the atomic structure of the molecule on the surface is fixed rigidly; this gives rise to the enhanced atomic contrast over the benzene rings in comparison with experiment.

Finally we compare the different channels (AFM, STM, and IETS) calculated with our simulation model, including the electrostatic distortion correction considering the probe particle with a negative charge of $-0.4e$. Figure 4(a) illustrates the relaxation of the probe particle due to the interaction with the surface, which is responsible for the distortion and sharpening of AFM/STM images as discussed in Refs. [6,8]. In the far distance regime, where the probe particle does not relax, the molecular contrast is blurred in all channels. The situation changes when the probe particle starts to move towards the local minima of the surface potential, producing the sharpening of both the STM and AFM contrasts, followed by the characteristic AFM signal inversion between the atoms or bonds and the rings [8]. Simultaneously with the sharpening of the STM and AFM contrasts and the inversion of the AFM contrast we observe a considerable sharpening of the contrast in the IETS-STM channel, which unambiguously proves the importance of the probe particle relaxation also for the increased resolution observed in the experimental IETS-STM images.

We stress that the pattern of the calculated constant-height IETS-STM image at the far tip-sample distance $z = 8$ Å shown in Fig. 4(c) coincides very well with the

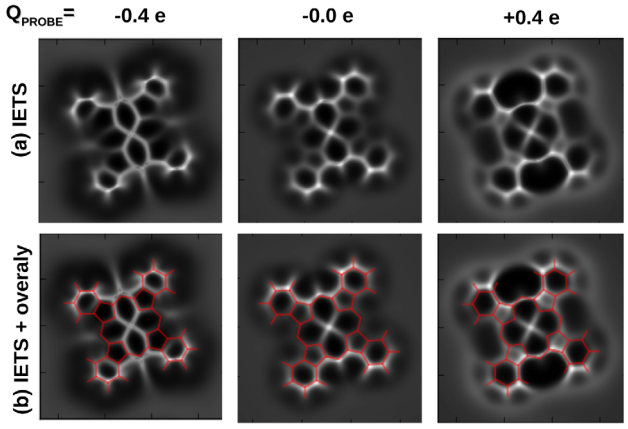

FIG. 3 (color online). Simulated constant-height IETS-STM images calculated at tip-sample distance $z = 7.3$ Å at $V = 1.5$ mV for different point charge values on the probe particle, $Q = -0.4e$, 0, and $+0.4e$. (a) IETS-STM images. (b) The same images as in panel (a), overlaid with the molecular skeleton (red line) of the relaxed CoPc molecule on Ag(110) obtained by the DFT calculations. Bright color indicates a large intensity of the IETS signal; see [29].

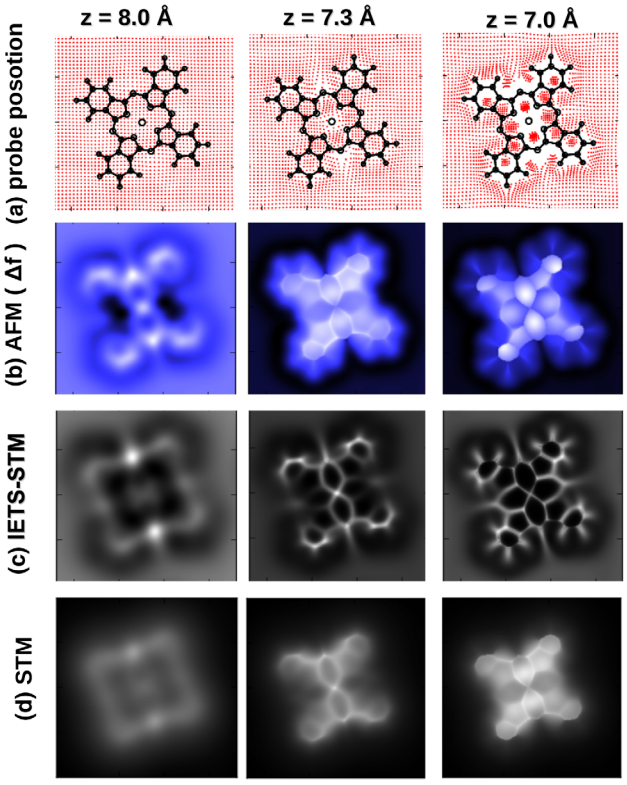

FIG. 4 (color online). Simulated constant-height AFM, STM, and IETS-STM images obtained with the extended simulation model assuming probe particle charge of $-0.4e$. (a) Red dots indicate the relaxed xy position of the probe particle; AFM (b), IETS-STM (c), and STM (d) channels for different tip-sample distances $z = 8.0$, 7.3, and 7.0 Å are shown. Color scales in all images except (a) are renormalized to obtain the best molecular contrast.

Hartree potential projected in the same z plane (see Fig. 3). This means that for these distances the shape of the tip-sample potential energy is determined mostly by the electrostatic interaction. Consequently, IETS-STM images acquired at far distances map directly the variation of the surface electrostatic potential at the given z.

To summarize, we have shown that the frustrated translation of the CO molecule at the tip apex reacts sensitively to the changes of local curvature of the surface potential. Namely, the attractive (convex) and repulsive (concave) character of the surface potential induces vibration mode hardening and softening, respectively. Detection of the resultant variations of the vibrational energy by the standard technique of IETS-STM allows one to map laterally the curvature of the surface potential. Since the curvature of the surface potential changes strongly in the vicinity of the atoms and interatomic bonds, the obtained maps are expected to be closely related to the underlying structure of the scanned surface. Furthermore, we have shown that the structural resolution obtained by lateral mapping of the IETS-STM signal is further sharpened by the lateral relaxations of the particle decorating the tip that occurs under the influence of the repulsive forces acting on it from the surface. This mechanism puts AFM, STM, and IETS-STM imaging with modified tips on a common ground. Finally, we have demonstrated that decorated tips can also be used to image local distributions of electrostatic charge. Eventually, this observation may be useful for the development and understanding of imaging techniques yielding better spacial resolution than the traditional AFM-based Kelvin probe force microscopy [19]. We believe that a detailed understanding of the IETS imaging mechanism and the influence of the internal charge distribution on the high-resolution images will contribute to further proliferate scanning probe microscopy techniques.

P. H. and P. J. acknowledge the support by GAČR, Grant No. 14-16963J and EMRP SIB611 CRYSTAL.

*Corresponding author.
hapala@fzu.cz
†jelinkep@fzu.cz

[1] R. Temirov, S. Soubatch, O. Neucheva, a. C. Lassise, and F. S. Tautz, New J. Phys. **10**, 053012 (2008).
[2] L. Gross, F. Mohn, N. Moll, P. Liljeroth, and G. Meyer, Science **325**, 1110 (2009).
[3] L. Bartels, G. Meyer, K.-H. Rieder, D. Velic, E. Knoesel, A. Hotzel, M. Wolf, and G. Ertl, Phys. Rev. Lett. **80**, 2004 (1998).
[4] C. Weiss, C. Wagner, C. Kleimann, M. Rohlfing, F. S. Tautz, and R. Temirov, Phys. Rev. Lett. **105**, 086103 (2010).
[5] G. Kichin, C. Weiss, C. Wagner, F. S. Tautz, and R. Temirov, J. Am. Chem. Soc. **133**, 16 847 (2011).
[6] L. Gross, F. Mohn, N. Moll, B. Schuler, A. Criado, E. Guitián, D. Peña, A. Gourdon, and G. Meyer, Science **337**, 1326 (2012).
[7] N. Pavliček, C. Herranz-Lancho, B. Fleury, M. Neu, J. Niedenführ, M. Ruben, and J. Repp, Phys. Status Solidi B **250**, 2424 (2013).
[8] P. Hapala, G. Kichin, C. Wagner, F. S. Tautz, R. Temirov, and P. Jelínek, Phys. Rev. B **90**, 085421 (2014).
[9] S. Kawai, A. Sadeghi, X. Feng, P. Lifen, R. Pawlak, T. Glatzel, A. Willand, A. Orita, J. Otera, S. Goedecker, and E. Meyer, ACS Nano **7**, 9098 (2013).
[10] M. Neu, N. Moll, L. Gross, G. Meyer, F. J. Giessibl, and J. Repp, Phys. Rev. B **89**, 205407 (2014).
[11] J. Welker and F. J. Giessibl, Science **336**, 444 (2012).
[12] Z. Sun, M. P. Boneschanscher, I. Swart, D. Vanmaekelbergh, and P. Liljeroth, Phys. Rev. Lett. **106**, 046104 (2011).
[13] I. Swart, L. Gross, and P. Liljeroth, Chem. Commun. (Cambridge) **47**, 9011 (2011).
[14] L. Gross, N. Moll, G. Meyer, R. Ebel, W. M. Abdel-Mageed, and M. Jaspars, Nat. Chem. **2**, 821 (2010).
[15] A. Riss, S. Wickenburg, P. Gorman, L. Z. Tan, H.-Z. Tsai, D. G. de Oteyza, Y.-C. Chen, A. J. Bradley, M. M. Ugeda, G. Etkin, S. G. Louie, F. R. Fischer, and M. F. Crommie, Nano Lett. **14**, 2251 (2014).
[16] M. P. Boneschanscher, S. K. Hämäläinen, P. Liljeroth, and I. Swart, ACS Nano **8**, 3006 (2014).
[17] C. Weiss, C. Wagner, R. Temirov, and F. S. Tautz, J. Am. Chem. Soc. **132**, 11 864 (2010).
[18] N. Moll, L. Gross, F. Mohn, A. Curioni, and G. Meyer, New J. Phys. **12**, 125020 (2010).
[19] F. Mohn, L. Gross, N. Moll, and G. Meyer, Nat. Nanotechnol. **7**, 227 (2012).
[20] R. C. Jaklevic and J. Lambe, Phys. Rev. Lett. **17**, 1139 (1966).
[21] B. C. Stipe, M. A. Rezaei, and W. Ho, Science **280**, 1732 (1998).
[22] J. I. Pascual, N. Lorente, Z. Song, H. Conrad, and H. P. Rust, Nature (London) **423**, 525 (2003).
[23] B. C. Stipe, M. A. Rezaei, W. Ho, S. Gao, M. Persson, and B. I. Lundqvist, Phys. Rev. Lett. **78**, 4410 (1997).
[24] S. Katano, Y. Kim, M. Hori, M. Trenary, and M. Kawai, Science **316**, 1883 (2007).
[25] B. C. Stipe, Science **279**, 1907 (1998).
[26] C. l. Chiang, C. Xu, Z. Han, and W. Ho, Science **344**, 885 (2014).
[27] G. Kichin, C. Wagner, F. S. Tautz, and R. Temirov, Phys. Rev. B **87**, 081408 (2013).
[28] See Supplemental Material at http://link.aps.org/supplemental/10.1103/PhysRevLett.113.226101 for more details, which includes Refs. [30–34].
[29] For simplicity we simulate the IETS signal as a gaussian peak in d^2I/dV^2 centered around the vibration energy ε with a fixed width $\sigma = 0.7$ meV, which fits well the experimental evidence.
[30] G. Kresse and J. Furthmüller, Phys. Rev. B **54**, 11 169 (1996).
[31] J. P. Perdew, J. A. Chevary, S. H. Vosko, K. A. Jackson, M. R. Pederson, D. J. Singh, and C. Fiolhais, Phys. Rev. B **46**, 6671 (1992).
[32] D. Vanderbilt, Phys. Rev. B **41**, 7892 (1990).
[33] S. Grimme, J. Comput. Chem. **27**, 1787 (2006).
[34] S. S. Batsanov, J. Mol. Struct. **990**, 63 (2011).